Evaluation of Alternative Altitude Scaling Methods for Thermal Ice Protection System in NASA Icing Research Tunnel

Sam Lee*
Vantage Partners, LLC, Cleveland, OH, 44135

Harold E. Addy, Jr.,† and Andy P. Broeren,‡
NASA Glenn Research Center, Cleveland, OH, 44135

and

David M. Orchard§
National Research Council, Ottawa, Canada

A test was conducted at NASA Icing Research Tunnel to evaluate altitude scaling methods for thermal ice protection system. Two new scaling methods based on Weber number were compared against a method based on Reynolds number. The results generally agreed with the previous set of tests conducted in NRCC Altitude Icing Wind Tunnel where the three methods of scaling were also tested and compared along with reference (altitude) icing conditions. In those tests, the Weber number-based scaling methods yielded results much closer to those observed at the reference icing conditions than the Reynolds number-based icing conditions. The test in the NASA IRT used a much larger, asymmetric airfoil with an ice protection system that more closely resembled designs used in commercial aircraft. Following the trends observed during the AIWT tests, the Weber number based scaling methods resulted in smaller runback ice than the Reynolds number based scaling, and the ice formed farther upstream. The results show that the new Weber number based scaling methods, particularly the Weber number with water loading scaling, continue to show promise for ice protection system development and evaluation in atmospheric icing tunnels.

Nomenclature

AIWT	=	Altitude Icing Wind Tunnel
h_G	=	Gas-phase convective mass transfer coefficient
K	=	Inertia parameter
K_0	=	Modified inertia parameter
IPS	=	Ice Protection System
IRT	=	Icing Research Tunnel
LWC	=	Liquid water content
M	=	Mach number
MVD	=	Median volumetric diameter
m_e	=	Evaporation rate
m_w	=	Water loading
P	=	Static pressure

* Engineer IV, Icing Branch, 21000 Brookpark Rd., MS 11-2, AIAA Senior Member.
† Aerospace Engineer, Icing Branch, 21000 Brookpark Rd., MS 11-2, AIAA Associate Fellow.
‡ Aerospace Engineer, Icing Branch, 21000 Brookpark Rd., MS 11-2, AIAA Associate Fellow.
§ Senior Research Officer, Aerospace, 1200 Montreal Road, M-17, AIAA Senior Member.

P_w = Partial pressure of vapor at free stream static conditions
P_{ww} = Partial pressure of vapor at the surface
Pr = Prandtl number
q_c = Convective heat transfer
q_{HA} = IPS heat input
r = Aifoil model leading edge radius
Re = Reynolds number
Re_{2r} = Reynolds number based on 2x leading edge radius
Re_δ = Reynolds number based on water droplet median volumetric diameter
T_r = Recovery temperature
T_s = Static temperature
T_{surf} = Surface temperature
T_t = Total temperature
We = Weber number
We_{DA} = Air density based Weber number
We_{DW} = Water density based Weber number
V = Airspeed
α = Angle of attack
δ = Water droplet median volumetric diameter
μ_a = Air viscosity
π_3 = Dimensionless scaling parameter (m_w/m_e)
ρ_a = Air density
ρ_w = Water density

I. Introduction

One of the most commonly used methods of ice protection on the leading edge aircraft wing is the thermal Ice Protection System (IPS). However, because this method is energy intensive, it is often operated as a "running wet" system where impinging water is not fully evaporated but allowed to runback and refreeze at non-critical locations. In order to evaluate a "running wet" system, accurate modelling of the entire icing process is required.

Currently most of the research and development of thermal ice protection systems is done in atmospheric icing wind tunnels that cannot simulate the effects of higher altitude at which these systems operate at. Therefore, the effects of higher altitude must be approximated using scaling techniques. Various methods of scaling for altitude effects have been proposed and used.[1,2,3,4] However, a better understanding of the processes involved in thermal IPS operation at altitude is needed to develop a validated and more widely accepted altitude scaling method.

National Aeronautics and Space Administration (NASA) and the National Research Council Canada (NRCC) conducted a joint research program to study the issues related to altitude scaling of thermal ice protection systems. NRCC provided test time in the Altitude Icing Wind Tunnel (AIWT) in Ottawa, Canada for three test campaigns in 2012, 2014, and 2015. The AIWT produces aircraft inflight icing conditions over a range of air speeds, temperatures, and pressure altitudes as well as inflight icing cloud densities and droplet sizes. NASA provided an 18-inch chord NACA 0018 model equipped with a simple piccolo tube heated-air IPS. The model was instrumented such that heated-air flow rates and temperatures as well as the surface temperatures of the leading edge could be monitored.

A. 2012 AIWT Campaign

The method used for the first AIWT campaign to scale test conditions so as to achieve similarity between altitude and ground level was based largely on a method that has some acceptance in the aviation industry.[1] Briefly, the method identifies four key scaling parameters, and then other test conditions were varied so as to keep the four key parameters constant between altitude and ground level. The four key parameters were: Reynolds number, water loading, inertia parameter, and recovery temperature.

This scaling method was investigated during the first AIWT campaign by using the tunnel's altitude capability to provide reference conditions to which the scaled conditions could be compared. The AIWT was run without its vacuum system operating to obtain the scaled conditions. Three sets of aircraft icing scenarios were selected for the tests. They were designated: Warm Hold, Cold Hold, and Descent.

Details of the first AIWT campaign are presented in Addy, et al.[5] A summary of the results is as follows:

1) Airfoil surface temperatures and thermal IPS heat energy use were well matched between altitude and corresponding ground-level conditions. This comparison was particularly good for dry-air conditions where the icing cloud was not activated but Reynolds-number matching dictated differing air speeds and air temperatures. The comparison was also very good for the wet-air conditions where the icing cloud was activated, but not as close as the dry-air conditions.
2) For two of the three scenarios, Warm Hold and Descent, the amount of ice accreted as well as its location on the airfoil was not well matched. For these scenarios, more ice was accreted at the ground-level cases and it froze farther aft on the airfoil surface. The Cold Hold results were somewhat inconclusive because difficulties during the test complicated execution of the reference and scaled cases for this scenario and other test priorities and limitations precluded repeating the test cases. Other complications arose in setting icing conditions in the tunnel for the Warm Hold and Descent scenarios which resulted in more uncertainty than was expected. The differences in the ice accretions for these scenarios were, however, more than could be explained by the increased uncertainty. The differences in ice mass and location were so pronounced that it was clear that the thermal IPS scaling method used was inadequate and unable to be effectively employed to accurately predict runback ice accretion when testing at ground-level conditions for at least a considerable range of flight scenarios.
3) During running-wet thermal IPS operation, water flowed aft in the form of drops and rivulets to areas where conditions permitted freezing. In these areas, both ice and liquid water were observed with the liquid water in the form of drops on top of the ice. Periodically, the drops would disappear. Instead of entirely evaporating or freezing in place, water may have been being re-entrained in the air flow. Such water transport had not been considered in the scaling method.

B. 2014 AIWT Campaign

The results of the initial test campaign indicated that matching Weber numbers between reference and scale was worthy of investigation. Several variations of the Weber number were considered during post-test analysis of the data. Because the Weber number based on air speed, density of water, and leading edge diameter showed best correlation with ice mass lost, it was used as a scaling parameter for the second test campaign.

Matching this form of the Weber number between altitude and ground-level conditions yielded scaled airspeeds that were close to the reference condition airspeeds. The resulting Reynolds numbers were much higher at ground-level than at altitude conditions and, therefore, the heat transfer from the airfoil surface to the exterior airflow was expected to be much higher than at the altitude condition. With higher heat transfer rates, lower airfoil surface temperatures and more freezing of runback ice was to be expected.

To counter the elevated convective heat transfer that was expected to occur, the heat energy provided by the thermal IPS was increased. This was done by increasing the thermal IPS air temperature and/or flowrate so as to match the airfoil leading edge surface temperatures when operating at the reference conditions. Since initial campaign results showed that Reynolds number scaling produced surface temperatures that are closely matched between altitude and ground level, surface temperatures obtained when operating at ground-level, Reynolds number-scaled conditions could also be used.

This scaling process, then, required two steps: 1) a test run with Reynolds number scaling to achieve heat transfer similarity and, therefore, surface temperatures for use in the second step and 2) a test run with Weber number scaling to get ice accretion similarity with a reset thermal IPS to obtain the surface temperatures of the first step. The Weber scaling step assumed water re-entrainment is a major contributor to the difference in accreted ice between reference and Reynolds number scaled conditions as was seen in the initial tests. For each step, scaling of water loading, inertia parameter, and recovery temperature were done to ensure similarity of these parameters to the reference conditions. They have no significant effect on either Reynolds or Weber numbers.

The second AIWT campaign, then, consisted of tests run at altitude, Reynolds number-scaled, and Weber number-scaled with surface temperature matched conditions. Like the first campaign, Warm Hold, Cold Hold, and Descent icing scenarios were used to set reference conditions. Details of the second campaign and discussion of the test are given in Addy, et al.[6] In summary, the results of the second campaign were:

1) As was the case in the initial test campaign, Reynolds number scaling produced close matching of airfoil surface temperatures, heated air inlet and outlet temperatures, and energy use rates between the reference and scaled conditions. This showed again that the Reynolds number scaling method works well in matching the heat transfer between altitude and ground level conditions.

2) Use of Weber number scaling produced ice accretions that were much closer, in terms of amount, location, and shape of ice, to those formed at the reference or altitude conditions. The Weber number based on the density of water was used in this test campaign. Airfoil surface temperatures were also matched between reference and scale conditions through the increase of heat energy supplied by the IPS.
3) This Weber number scaling method requires two steps when using an atmospheric icing wind tunnel: the first step is running at Reynolds number scaled conditions to determine the correct (altitude) surface temperatures. The second step is to run at Weber number scaled condition while adjusting the IPS to match the surface temperatures obtained in step one.
4) The increased heat transfer occurring at Weber number scaling conditions does, however, have an effect on the runback ice formation, particularly at low air temperatures such as those of the cold hold icing scenario. The ice freezes further forward on the model, but is not well adhered to the model surface that is being warmed underneath by the IPS.
5) The new, two-step altitude scaling method evaluated as part of the second campaign provided a way of evaluating both the heat transfer and mass transfer performance of a thermal ice protection system that does not rely on the application of empirical correction factors, but instead relies on the straightforward application of the primary physics involved.

C. 2015 AIWT Campaign

Results from the second AIWT campaign showed that Weber number was an important parameter for scaling aircraft icing conditions between altitude and atmospheric icing wind tunnel pressures. The test data were then further examined with the intent of finding other similarity parameters that may be of significance. In addition to water droplet re-entrainment, water evaporation from a heated aircraft surface at altitude is a mode of mass transport to consider further. Like water re-entrainment, there is no method available to experimentally measure the amount or rate of water evaporation during IPS operation in aircraft icing conditions. A physical relationship that has been used for quite some time in performing mass balance calculations for unprotected surfaces in icing condition is:

$$m_e = h_G \left(\frac{P_{ww} - P_w}{P} \right)$$

where m_e is the mass of water evaporated, h_G is the gas-phase convective mass transfer coefficient, P_{ww} is the partial pressure of water vapor at the surface, P_w is the partial pressure of water vapor at free stream static conditions, and P is the static pressure. Although it has been noted that this equation may not be valid for heated surfaces, there is no reason to believe that it may not be a reasonable approximation.

To form a non-dimensional similarity parameter, the ratio of water loading to mass evaporation was used. Full details of the analysis of the data from the second campaign are given in Orchard, et al.[7] In the post-test analysis of the second AIWT campaign, a relationship between the ratio of water loading to water evaporation and the rate of ice accretion was found. Further analysis of the data considered convective heat transfer from the surface and Weber number based on air density. Ice accretion rate was found to be proportional to a factor composed of the ratio of water loading to water evaporation, convective heat transfer, and Weber number based on air density.

In a separate, parallel investigation,[7] dimensional analysis was used to find other parameters that may be of importance in scaling icing conditions for thermal IPS testing in atmospheric wind tunnels. The investigation started by assuming that ice accretion rate was a function of thirteen variables: airspeed, water loading, leading edge diameter, total temperature, surface temperature, air density, convective heat transfer, heat energy from IPS, air viscosity, surface tension of water, water evaporation, and dynamic pressure. A conventional dimensional analysis technique was used in conjunction with prior test results to produce the following dimensionless parameters of significance:

1) $\pi_1 = We_{DA}$
2) $\pi_2 = Re$
3) $\pi_3 = m_w/m_e$
4) $\pi_4 = q_c/q_{HA}$
5) $\pi_5 = T_{surf}/T_t$

Of these parameters, π_1, π_2, π_4, and π_5 were taken into account in the first two campaigns. In those campaigns, however, water loading, m_w, was used by itself as a scaling parameter and held constant between altitude and ground level conditions. For many years in situations where scaling of icing conditions is necessary, it has been recognized that water loading must be constant between the reference and scaled condition in order to achieve icing similarity. The idea of scaling it so as to keep the ratio of m_w / m_e is new. It provides a means by which the increased water evaporation occurring at altitude conditions may be compensated for in an atmospheric icing tunnel.

This new scaling method (*WePi3)*, then, matches inertia parameter, recovery temperature of the air stream, model surface temperatures, Weber number based on air density, and the ratio of water loading to water evaporation. A two-step sequence of first matching Reynolds numbers to obtain target surface temperatures on the model would need to be used in an atmospheric tunnel. This scaling method was tested in the third AIWT test campaign. Again, a set of reference icing flight scenarios, designated Warm Hold, Cold Hold, and Descent, were used. Details of this test campaign are given in Orchard, et al.[7] A summary of the results is presented below:

1) Results showed that the new scaling method, using matched We_{DA} and π_3, yielded ice accretions similar to those accreted at altitude conditions; much better than those accreted using the *Re* scaling method. The ice accretions formed using the We_{DA} and π_3 showed about the same agreement with those formed at altitude conditions as did the ones formed using the We_{DW} method used during the second AIWT campaign. There was, however, less of an effect on the ice of enhanced cooling in the Cold Hold scenario due to the lower Reynolds numbers generated using We_{DA} matching instead of We_{DW}.
2) The agreement in ice accretions between scaled and altitude conditions indicated that scaling water loading is a valid technique.
3) Photographs of ice accretions showing strong evidence that water droplet re-entrainment does occur was documented.

D. 2016 IRT Campaign

The tests conducted at AIWT were very valuable in developing and evaluating various altitude scaling methods for thermal ice protection systems, as well as developing a better understanding of the processes involved in runback icing and their relative importance. A follow-on test was conducted in NASA Icing Research Tunnel using a much larger business jet-class airfoil model and an ice protection system more similar to those found in commercial aircraft. This paper presents the results of the test conducted in the IRT.

The IRT is an atmospheric tunnel that cannot simulate altitude (reference) conditions. Therefore, ice accretions obtained using the various scaling methods cannot directly be compared to those obtained at the reference conditions. However, the ice shapes from the various scaling methods are compared to one another, and the trends were compared to the results observed in AIWT tests where the altitude reference conditions were run.

II. Experimental Setup

The test was conducted in the Icing Research Tunnel (IRT) at NASA Glenn Research Center in Cleveland, Ohio. The test section has width of 9 ft., height of 6 ft., and length of 20 ft. It is capable of speeds of up to 390 mph and the test section total temperature can be controlled between of -20° to 33° F. It is capable of generating a significant portion of FAA Appendix C icing envelope. More details on the facility can be found in Soeder, et al.[8]

A. Model

The model used for this study was a 60-inch chord, 72-inch span 2D airfoil representative of a modern business jet, as shown in Fig. 1. It was built and used in 2006 in the IRT as part of an IPS analysis and modelling study performed by the Wichita State University under grants from the FAA and NASA.[4] The model was constructed out of aluminum with the outside surface polished to a mirror finish. It was fabricated with two removable leading edges: an unheated leading edge and a heated leading edge. The unheated leading edge was instrumented with surface pressure taps for aerodynamic measurements. The heated leading edge contained a piccolo tube ice protection system as well as instrumentation for thermal studies. The holes on the piccolo tube were arranged in a diamond pattern, and the diffuser section was backed by an inner-liner skin, as shown in Fig. 2. The hole pattern extended 5.5 ft. of the length of the piccolo tube. The skin was constructed out of a single sheet of aluminum and had a thickness of 0.10 in.

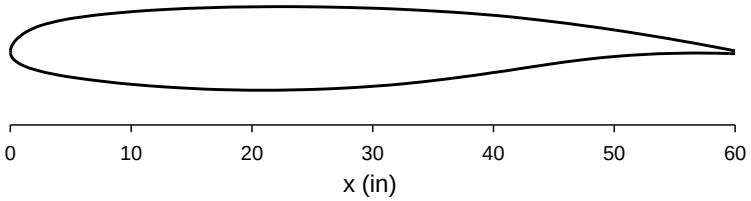

Figure 1. Business jet model coordinates.

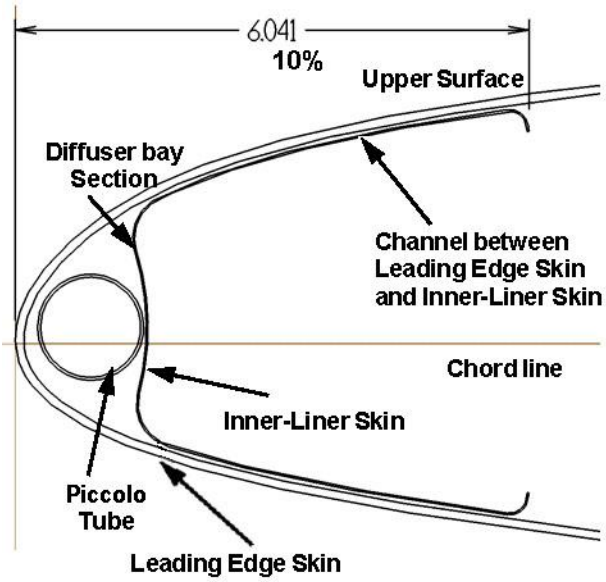

Figure 2. IRT model ice protection system cross section. (from Papadakis, et al.[4])

The model was mounted vertically in the test section on the turntable that was used to set the angle of attack, as shown in Fig. 3. The IRT hot air system provided the preheated pressurized air for the piccolo tube as shown in Fig. 4. A Micromotion CMF200M coriolis mass flow meter was used to measure the heated air flow rate. An electric heater located just below the tunnel floor was used to accurately control the inlet temperature of the piccolo tube.

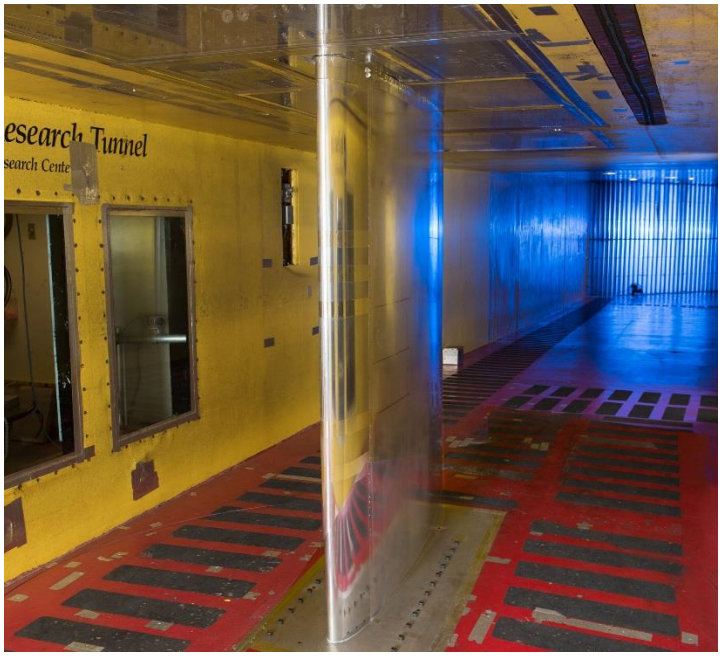

Figure 3. Business jet model ice in IRT test section.

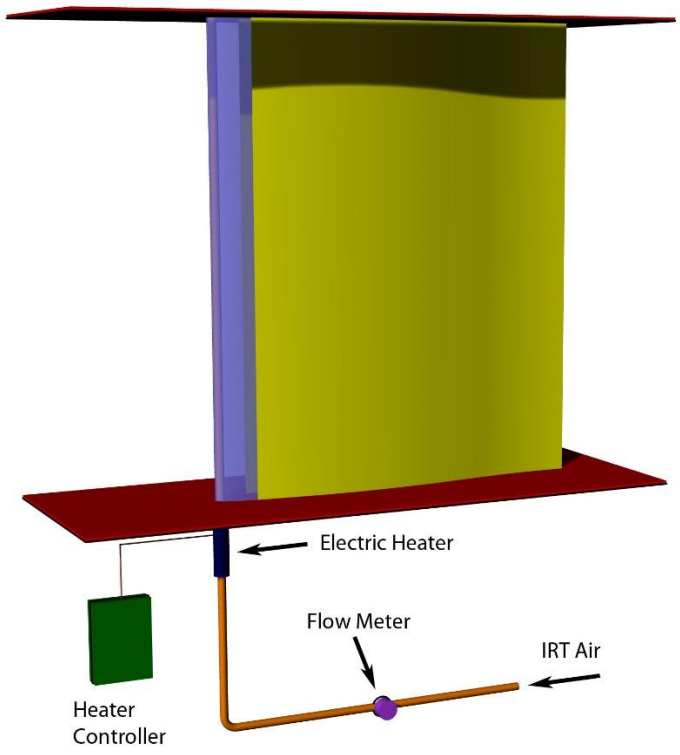

Figure 4. Model heated air supply line and instrumentation.

The model was originally designed to be used for heated air thermal ice protection system analysis and to generate experimental data for computational code study. The heated leading edge was, thus, extensively instrumented with

temperature and pressure sensors. However, since this was not the purpose of the test described in this paper, only the instrumentations that were relevant for this study are described in detail here. A detailed description of the full instrumentation suite on the model can be obtained in Papadakis, et al.[4] There were surface pressure taps along the midspan of the model (on the main part of the model as well as the unheated leading edge) used to fine tune the model angle of attack. The surface temperatures on the heated leading edge were obtained from a chordwise row of 32 type-T thermocouples located 30.175" from the tunnel floor, as shown in Fig. 5. The IPS inlet temperatures were obtained by averaging four type-T thermocouples located in the piccolo tube at 6.92", 30.18", 42.43", and 65.69" from the floor. The IPS outlet temperatures were obtained by averaging four type-T thermocouples located in the diffuser (or air return) section behind the inner liner skin at 12", 33.5", 40", and 60" from the floor.

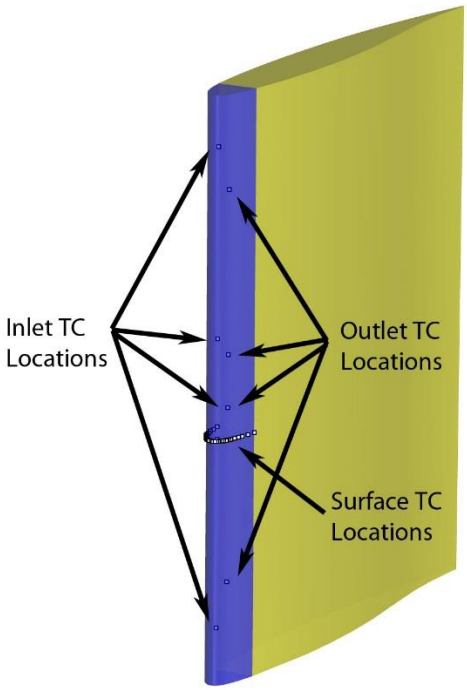

Figure 5. Heated leading edge thermocouple instrumentation layout.

B. Test Conditions

Three flight icing scenarios served as the reference conditions for the study. These were:

1) Descent
2) Cold hold
3) Warm Hold

The conditions for these scenarios are given in Table 1. These conditions were identical to those used in the AIWT tests, except for the angle of attack. The asymmetric airfoil and IPS used in this test called for varying the angle of attack to match the corresponding icing scenarios. The scaled conditions were obtained by reducing the altitudes shown in Table 1 to the tunnel altitude and scaling the icing parameters while maintaining the parameters shown in Table 2 constant. For the *Re*-based scaling method, the Reynolds number, water loading, modified inertia parameter, and recovery temperature were kept constant. For the We_{DA}-based scaling method, air density based Weber number, water loading, modified inertia parameter, and recovery temperature were kept constant. For the *WePi*3-based scaling method, the air density-based Weber number, $\pi 3$ mass ratio, modified inertia parameter, and recovery temperature were kept constant.

Table 1. Reference conditions

Flight Phase	Altitude (ft)	V (kts)	α (deg)	T_s (deg C)	T_t (deg C)	LWC (g/m^2)	MVD (μm)
Descent	10000	180	-1	-14.2	-10	0.35	19.1
Cold Hold	15000	180	3	-20.1	-15.8	0.24	17.5
Warm Hold	15000	180	3	-8.6	-4.3	0.49	17.4

Table 2. Scaling parameters held constant

Scaling Method	Scaling Parameters Held Constant			
Re	Re_{2r}	m_w	K_0	T_r
*WePi*3	*WeDA*	m_w	K_0	T_r
WeDW	*WeDW*	*Pi*3	K_0	T_r

The equations used to calculate these parameters were as follows:

$$Re_{2r} = \frac{\rho_a \cdot V \cdot 2r}{\mu_a} \tag{1}$$

$$m_w = \mathrm{LWC} \cdot V \cdot \beta_0 \tag{2}$$

where:

β_0 = collection efficiency at stagnation

$$K_0 = \frac{1}{8} + \frac{\lambda}{\lambda_{\mathrm{Stokes}}}\left(K - \frac{1}{8}\right) \tag{3}$$

where

$$K = \frac{\rho_w \cdot \delta^2 \cdot V}{18(2r)\mu_a}$$

and

$$\frac{\lambda}{\lambda_{\mathrm{Stokes}}} = \frac{1}{0.8388 + 0.001483 Re_\delta + 0.1847\sqrt{Re_\delta}}$$

and

δ = droplet median volumetric diameter

$$T_r = T_s\left(1 + \sqrt{Pr}\left(\frac{\gamma - 1}{2}\right)M^2\right) \tag{4}$$

$$We_{DW} = \frac{\rho_w \cdot V^2 \cdot (2r)}{\sigma_w} \tag{5}$$

where:

σ_w = surface tension of water

$$We_{DA} = \frac{\rho_a \cdot V^2 \cdot (2r)}{\sigma_w} \tag{6}$$

$$\pi_3 = m_w/m_e \tag{7}$$

where:

$$m_e = h_G \left(\frac{P_{ww} - P_w}{P} \right)$$

More detailed description of these scaling methods can be found in Addy, et al.[5,6] and Orchard, et al.[7]

C. Experimental Uncertainties

The IRT was calibrated to generate LWC and MVD within 10% of the stated values. The thermocouples used for the surface temperature measurements and the IPS inlet/outlet temperatures had an accuracy of 1° C. The flow meter used to measure the heated air mass going into the IPS had a manufacturer-stated accuracy of 0.35%.

D. Test Procedure

For runback water to freeze in a manner similar to that at altitude, one of the conditions that needs to be met is that model surface temperatures need to be similar to those occurring at altitude. With the IPS operating at the same heated air mass flowrate and temperature, Reynolds number scaled conditions result in model surface temperatures nearly identical to those during operation at altitude conditions. This is generally true for both dry air and icing conditions, but more so for dry air. Because of this, the surface temperatures obtained at *Re*-scaled conditions could also be used as reference values.

When operating at Weber number scaled conditions, however, convective cooling by the tunnel airstream is elevated, resulting in a different model surface temperature profile. To compensate for the enhanced convective cooling, IPS system output is increased in temperature, mass flow rate, or both, to obtain the correct model surface temperature. Therefore, Weber number scaling methods require two steps: first run at Reynolds number scaled conditions to obtain the reference model surface temperatures, then run at Weber number scaled conditions adjusting the IPS system to get the model surface temperatures obtained in step one. These two steps are performed with dry air in the tunnel. The icing run may then commence at the Weber number scaled conditions to obtain runback icing results similar to those that would be expected at altitude.

Once the IPS parameters for the test were obtained, tests were done using the various scaling methods described in the introduction. The following describes the typical test procedure:

1) Set IPS air mass flow rate and temperature to obtain "reference" (*Re*-scaled) model leading edge temperature.
2) Activate icing spray for a predetermined icing exposure time.
3) Shut tunnel down and document the ice accretion using photographs. Perform 2D ice tracings, ice thickness measurements, and ice mass measurements. Record frozen rivulets using BIO-FOAM impression block.

The ice tracings were obtained by tracing the outline of the ice shape on a cardboard with the leading edge of the airfoil cut out. The tracings were then digitized using a 2D scanner. Ice mass measurements were obtained by scraping the ice off the model (over a fixed amount of model span) onto a tray and weighing it. The rivulet impression was obtained by pressing a block of BIO-FOAM (with the airfoil contour cut out) on the model surface. BIO-FOAM a closed-cell compressible foam typically used in the medical industry to obtain orthotic and podiatric impressions. However, because of its low thermal mass and high compressibility, it has been shown to be useful in obtaining impressions of runback ice shapes.[6] The impression could then be digitized using a 3D laser scanner. The laser scan data of the BIO-FOAM were not available in time for this paper, but will be included in a follow-on report.

III. Results and Discussion

The ice accretion and IPS thermal data from Descent, Cold Hold, and Warm Hold flight scenarios with *Re* and *We* based scaling methods are presented in this section. The results from the different scaling methods are compared to each other and also with the trends observed in the AIWT tests.

A. Descent Scenario

Table 3 shows the reference conditions, scaled test conditions, scaling parameters, and the accreted ice mass for the Descent scenario. The differences in altitude for the scaled conditions were due to a variation in the static pressure at different airspeeds (since the pressure cannot be directly controlled in an atmospheric wind tunnel). The *Re*-based scaling method resulted in ice mass that was approximately twice as large as the two *We*-based scaling methods. This was similar to results from the AIWT tests[6,7] where ice accretions for the Reynolds number scaled conditions were always much larger than those produced at the Weber number scaled conditions, as well as those produced at the reference, or altitude, conditions.

Table 3. Descent scaled test conditions and ice mass.

Scale Method	Alt (ft)	V (kts)	T_s (deg C)	LWC (g/m^3)	MVD (μm)	Spray Time (s)	m_w (g/m^2s)	Re_{2r} ($x10^6$)	WeDA	Pi3	WeDW ($x10^6$)	Ice Mass (g)
Reference	*10000*	*180*	*-14.2*	*0.35*	*19.1*	*360*	*17.6*	*0.224*	*5814*	*1.62*	*6.21*	*N/A*
Re	1066	133	-12.7	0.48	22.8	360	17.6	0.224	4315	2.24	3.38	20
WePi3	1439	159	-13.5	0.35	19.4	360	14.4	0.265	5814	1.62	4.84	8.5
WeDW	1782	180	-14.2	0.34	21.6	360	17.6	0.297	7769	1.88	6.21	12.7

Figure 6 shows the cross section cuts of the ice shapes for the Descent scenario, and Figure 7 shows the photos of the accreted ice on the upper surface. Although photos of the lower surface ice accretion were taken during the test, only the upper surface photos are presented in this paper for brevity since ice contamination on the upper surface is much more significant aerodynamically than on the lower surface. Figures 6 and 7 both show that runback ice for the *Re*-scaling condition started and extended farthest downstream. During the AIWT tests, both *We*-based scaling methods produced ice very similar to that of the reference conditions in terms of the location on the airfoil, extent, and height, while the *Re*-scaled ice accretion started farther downstream, had greater height and much greater chordwise extent than either the *We*-based scaled ice shapes or the reference ice shape. Of note here is that, in the IRT test, the We_{DW} scaled ice started slightly upstream of the *WeP*i3 scaled ice. The two *We*-scaled ice accretions in the AIWT tests were recorded in separate test entries and were not directly comparable. However, both ice accretions started on the airfoil at very nearly the same locations on the airfoil as the reference ice.[6,7]

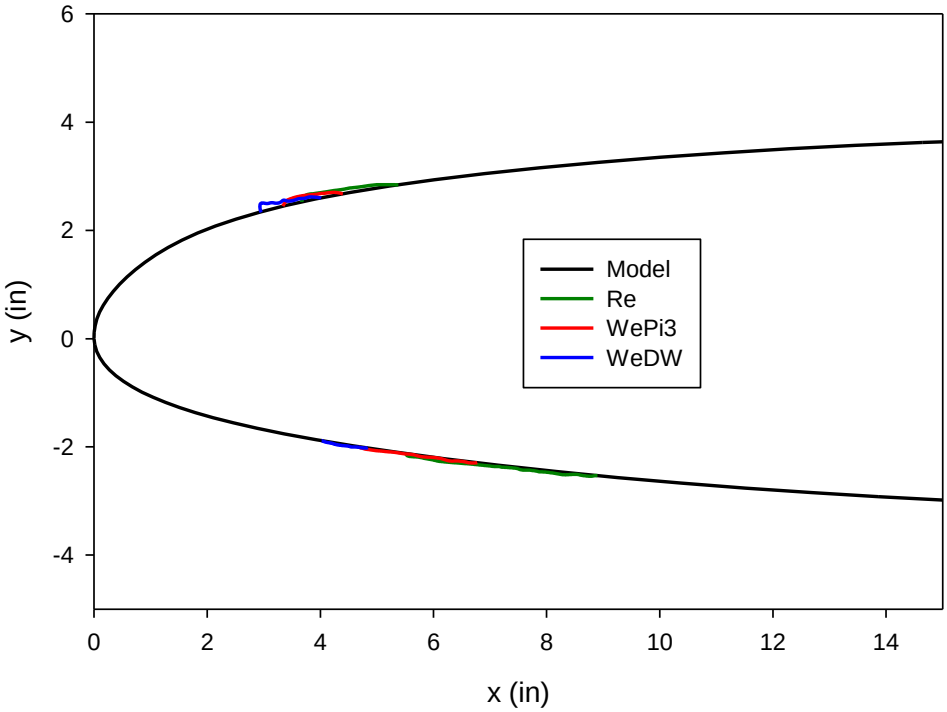

Figure 6. Descent scenario ice accretion tracing.

a) *Re* scaling **b) *WePi*3 scaling** **c) We_{DW} scaling**

Figure 7. Descent scenario upper surface ice accretion.

The chordwise surface temperature distribution for the Descent scenario is shown in Fig. 8 for both spray off (dry) and spray on (wet) conditions. There was an approximately 25° C temperature drop when the spray was turned on. When the spray was off, the leading edge temperature for all three scaling methods were matched nearly identically (since the IPS settings were set so that the leading edge temperatures were matched). Away from the leading edge, there were some small differences in the temperature due to differences in convective cooling rates. The *Re*-based

scaling method had the warmest temperature since it had the lowest Reynolds number, and the We_{DW}-based scaling method had the coolest temperature since it had the highest Reynolds number. Similar trends were also observed when the spray was turned on.

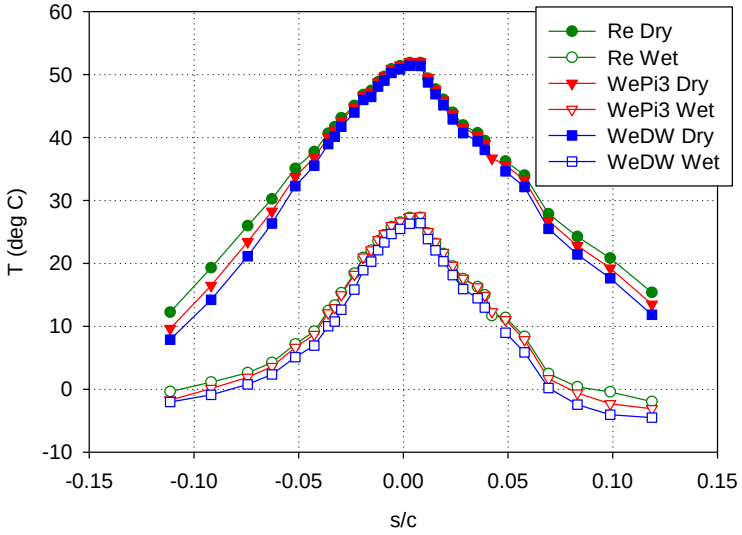

Figure 8. Descent scenario leading edge surface temperature.

Figure 9a shows the IPS heated air inlet/outlet temperatures, and Figure 9b shows the IPS heated air energy input rates. The *Re*-scaling IPS inlet temperatures and energy input should be nearly identical to the reference condition values (as was shown in the AIWT tests) had it been possible to run the reference conditions in the IRT. The inlet temperatures and energy input from both of the *We*-based scaling method were higher than the *Re*-based scaling values since increased thermal energy (in the form of higher inlet temperature) was required to maintain the leading edge temperature at higher Reynolds number. The differences were much less in the outlet temperature between the *Re*-based and *We*-based scaling methods. Similar results were obtained during the AIWT tests.

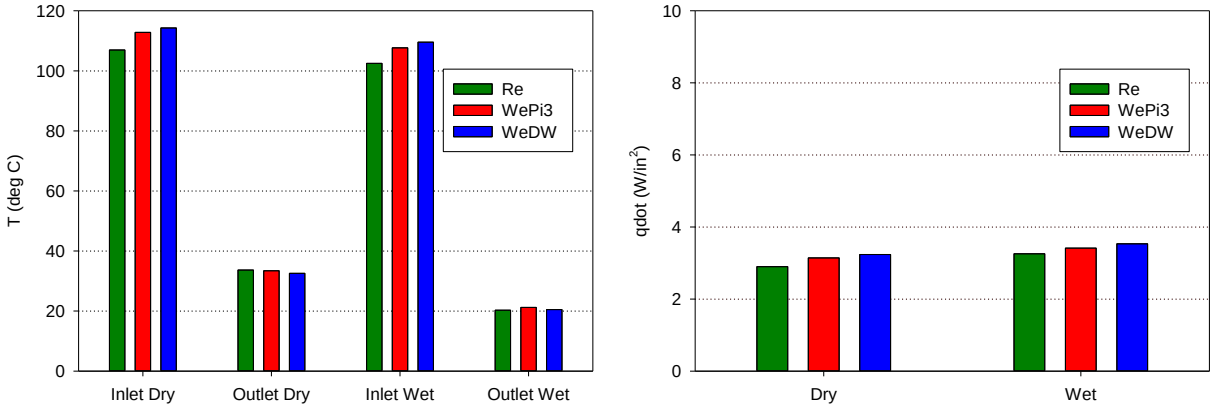

a) Heated air inlet/outlet temperature **b) Heated air energy input**

Figure 9. Descent scenario heated air temperature and energy input before and during icing exposure.

B. Cold Hold Scenario

The test conditions and the accreted ice mass for the Cold Hold scenario are shown in Table 4. The reference condition was slightly modified from that shown in Table 1 in order to run the *Re* scaled condition at calibrated IRT LWC and MVD point for more precise values (since these values are interpolated with uncertainties of up to ±10% away from the calibrated points). The accreted ice mass for the *Re*-based scaling method was almost 11 times higher than the *WePi*3-based scaling method. The accreted ice for the We_{DW}-based scaling method shed during the icing run, so only a partial mass was obtained. It was notable that the ice accretion also shed for the We_{DW}-based condition during the AIWT test.[5]

Table 4. Cold Hold scenario scaled test conditions and ice mass. (*Ice shed during test)

Scale Method	Alt (ft)	V (kts)	T_s (deg C)	LWC (g/m^3)	MVD (μm)	Spray Time (s)	m_w (g/m^2s)	Re_{2r} ($x10^6$)	WeDA	Pi3	WeDW ($x10^6$)	Ice Mass (g)
Reference	*15000*	*185*	*-20.1*	*0.31*	*14.6*	*600*	*13.4*	*0.193*	*5147*	*1.06*	*6.54*	*N/A*
Re	976	109	-16.4	0.52	20.1	600	13.4	0.193	3065	1.87	2.27	54.2
WePi3	1495	149	-16	0.28	16.9	600	9.5	0.253	5147	1.06	4.22	5.0
WeDW	2087	185	-15.7	0.27	18.9	600	13.3	0.31	8346	1.37	6.54	16.4*

Figure 10 shows the cross section cuts of the ice shapes for the Cold Hold scenario. Figure 11 shows the photos of the accreted ice on the upper surface. They show that again the runback ice for the *Re*-based scaling started and extended farthest downstream. The ice shape for the We_{DW} scaled condition again started farthest upstream.

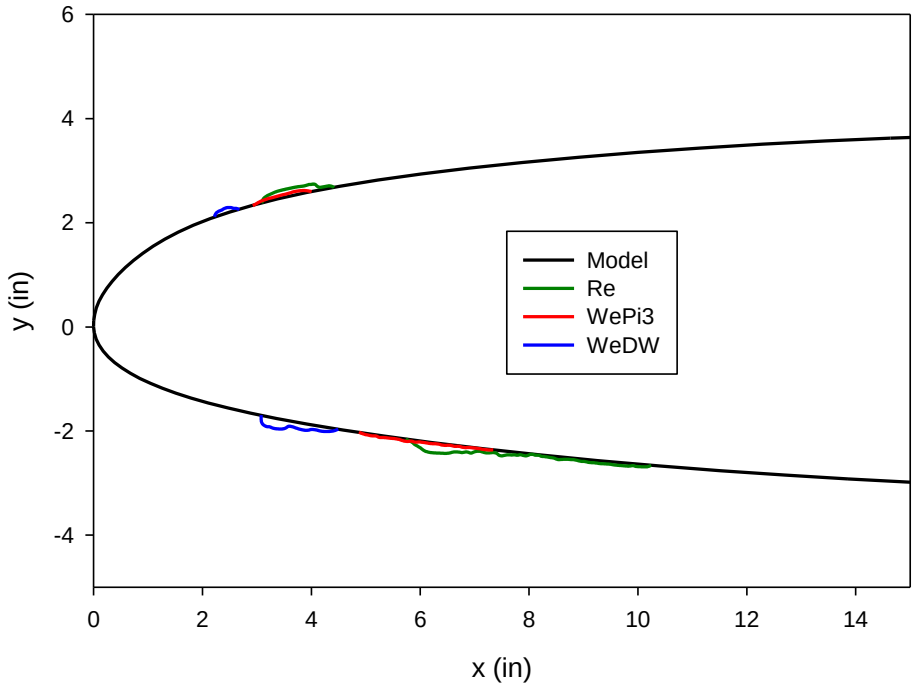

Figure 10. Cold Hold scenario ice accretion tracing.

a) *Re* scaling **b) *WePi*3 Scaling** **c) We_{DW} Scaling**

Figure 11. Cold Hold scenario upper surface ice accretion.

The chordwise surface temperature distribution for the Cold Hold scenario is shown in Fig. 12. When the spray is off, the leading edge temperature for all three scaling methods were matched nearly identically. When the spray was turned on there was a slightly larger variation in the temperature profile between the three scaling methods, with the *WePi*3 method being the warmest and We_{DW} method being the coldest.

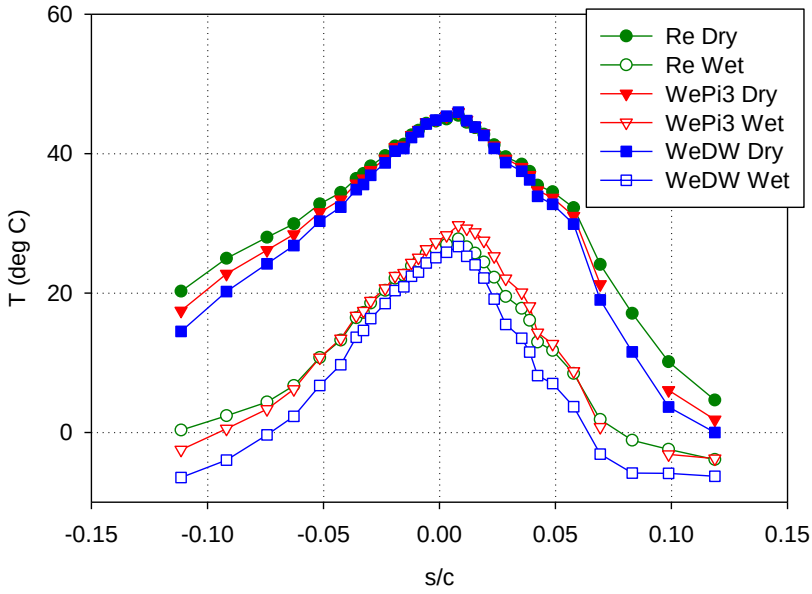

Figure 12. Cold Hold scenario leading edge surface temperature.

Figure 13 shows the IPS heated air inlet/outlet temperatures and the IPS heated air energy input rates. The *Re*-scaling IPS inlet temperatures and energy input were the lowest, followed by the *WePi*3 method and the We_{DW} method. Similar results were obtained with the Cold Hold scenario during the AIWT tests.

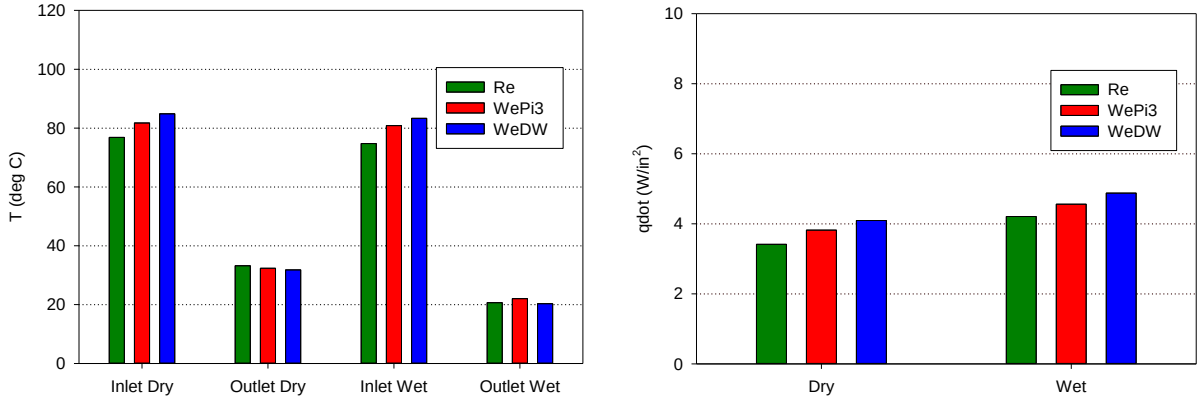

a) Heated air inlet/outlet temperature **b) Heated air energy input**

Figure 13. Cold Hold scenario heated air temperature and energy input before and during icing exposure.

C. Warm Hold Scenario

Table 5 shows the reference and scaled test conditions as well as accreted ice mass for the Warm Hold scenario. As with the Cold Hold scenario, the reference condition was slightly modified from what is shown in Table 1 in order to obtain a more accurate *Re*-based test condition. Figure 14 shows the cross section cuts of the ice shapes taken from tracings at the centerline of the model, and Fig. 15 shows the photos of the accreted ice on the upper surface. Again, a much greater amount of ice was formed at the *Re*-based scaled conditions. As the ice tracings in Fig. 14 show, the ice again started much farther downstream and had a much greater chordwise extent. As has been noted, this is the same trends as observed in the AIWT tests where the *We*-based scaling methods resulted in ice accretions much closer

to the reference ice shapes. Of note here though, is the starting location and shape of the We_{DW} ice accretion. It again started further upstream than for the other methods. In addition, the lower surface ice formed a prominent ridge not seen in the other scaling methods or during the AIWT tests. For all three scaling methods, the increased angle of attack (when compared to AIWT tests) caused an increase in the water loading on the lower surface. It was possible the combination of the increased water loading and the high Reynolds number of the We_{DW} condition resulted in the formation of a lower-surface ridge.

Table 5. Warm Hold scenario scaled test conditions and ice mass.

Scale Method	Alt (ft)	V (kts)	T_s (deg C)	LWC (g/m^3)	MVD (μm)	Spray Time (s)	m_w (g/m^2s)	Re_{2r} ($x10^6$)	WeDA	Pi3	WeDW ($x10^6$)	Ice Mass (g)
Reference	*15000*	*185*	*-8.6*	*0.39*	*18.3*	*1260*	*20.0*	*0.186*	*4922*	*1.74*	*6.55*	*N/A*
Re	1336	109	-6.3	0.66	25.4	1260	20.0	0.186	2923	3.09	2.26	207.5
WePi3	1814	147	-7.3	0.36	19.6	1260	13.6	0.241	4922	1.74	4.12	64.5
WeDW	2454	184	-8.6	0.37	22	1260	20.0	0.299	8005	2.24	6.55	138.8

Figure 15 shows that there was a significant spanwise variation on where the runback ice started for the We_{DW} condition, which was not observed for the *Re* and *WePi*3 cases. In addition to the increased convective cooling caused by the higher tunnel airspeed and slightly increased IPS operating temperature required for this scaling method, the icing cloud generally becomes less uniform in the tunnel as the airspeed is increased, possibly explaining some of this variation.

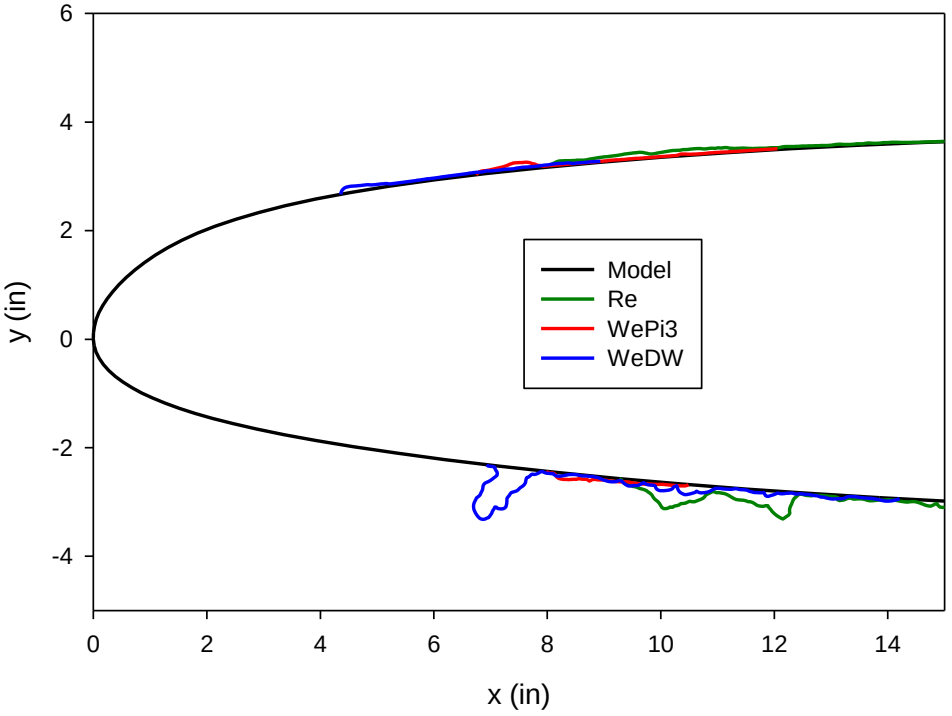

Figure 14. Warm Hold scenario ice accretion tracing.

a) *Re* scaling **b) *WePi*3 scaling** **c) We_{DW} Scaling**

Figure 15. Warm Hold scenario upper surface ice accretion.

Figure 16 shows the chordwise surface temperature distribution for the Warm Hold scenario. Similar to the other two scenarios, when the spray was off, the leading edge temperature for all three scaling methods were matched nearly identically. Away from the leading edge, there were some slight differences in the temperature due to differences in convective cooling rates. Similar trends were also observed when the spray was turned on.

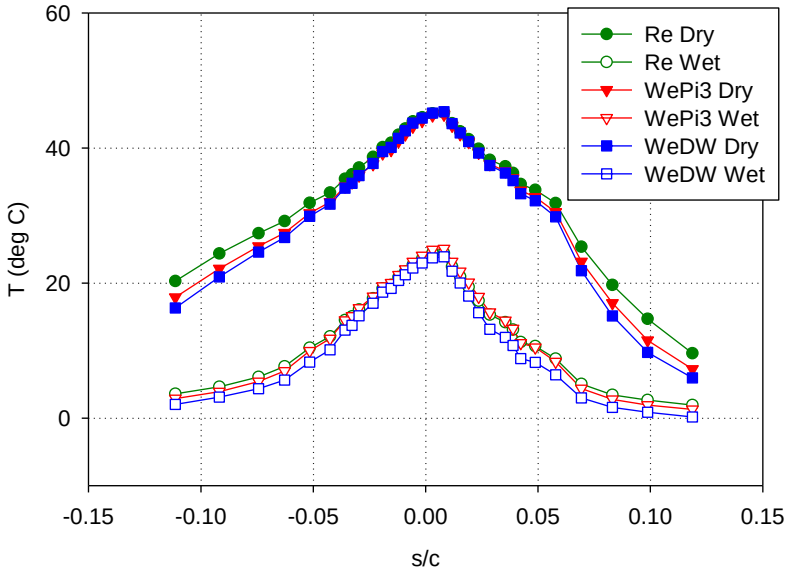

Figure 16. Warm Hold scenario leading edge surface temperature.

The IPS heated air inlet/outlet temperatures and heated air energy input rates for the Warm Hold scenario are shown in Fig. 17. Both of the *We*-based scaling inlet temperatures and energy input were higher than the *Re*-based scaling values, with the We_{DW}-based scaling method being slightly higher than the *WePi*3-based scaling method. This was very similar to what was observed for the other scenarios.

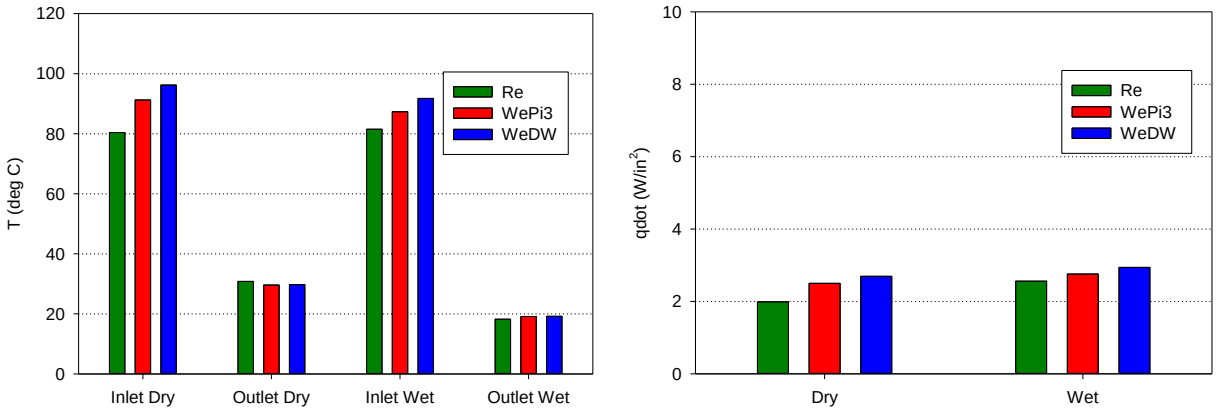

a) Heated air inlet/outlet temperature **b) Heated air energy input**

Figure 17. Warm Hold scenario heated air temperature and energy input before and during icing exposure.

D. WSU Warm Hold Scenario

To enhance the test, another reference scenario was added to the IRT test matrix that was not run at the AIWT. The Warm Hold WSU was a condition that was tested during the 2006 WSU test in the IRT.[4] This provided an additional Warm Hold scenario at a higher speed than what was used in AIWT (since that facility was limited to 180 knots). Table 6 shows the test conditions and the accreted ice mass for the Warm Hold WSU scenario. The reference airspeed for this scenario was 205 knots, compared to the 180 knots of the Warm Hold scenario shown in Table 1, resulting in higher Reynolds number. In addition to the *Re*, *WePi*3, and We_{DW}-based scaling methods, the scaling method utilized during the WSU test was also used. The *Re*-based and WSU scaling conditions had similar Reynolds number that were lower than the two *We*-based scaling methods. The We_{DW} scaling method produced *Re* value 60% higher than the reference/Re-scaled conditions and 70% higher than the WSU scaling method. The *WePi*3-based scaling method had the lowest accreted ice mass (at approximately 30% of the *Re*-based scale value). The WSU-scaling method had the largest accreted ice mass, which was twice that of the *Re*-scaled method. For this particular scenario, the We_{DW}-based method had higher accreted ice mass than the *Re*-scaled method, which was not observed in AIWT tests or in the IRT Warm Hold scenario test at 180 knots.

Table 6. WSU Warm Hold scenario scaled test conditions and ice mass.

Scale Method	Alt (ft)	V (kts)	T_s (deg C)	LWC (g/m^3)	MVD (μm)	Spray Time (s)	m_w (g/m^2s)	Re_{2r} ($x10^6$)	WeDA	Pi3	WeDW ($x10^6$)	Ice Mass (g)
Reference	*15000*	*205*	*-9.4*	*0.5*	*20*	*1350*	*31.1*	*0.205*	*6065*	*1.73*	*8.04*	*N/A*
Re	1312	126	-6.3	0.82	27.2	1350	31.1	0.205	3769	2.98	3.01	236.5
WePi3	1835	164	-7.6	0.43	24	1350	21.0	0.264	6065	1.73	5.13	68.9
WeDW	2446	205	-9.2	0.5	22.4	1350	31.1	0.324	9715	2.23	8.04	266.2
WSU	1191	115	-9.4	0.87	29	1350	30.8	0.192	3229	3.03	2.53	483.3

Figure 18 shows the cross section cuts of the ice shapes for the WSU Warm Hold scenario. Figure 19 shows the photos of the accreted ice on the upper surface. These figures show that runback ice for the *Re*-based scaling method started farthest downstream, and the WSU-scaled ice accretion started farthest upstream. The *Re*-based method resulted in the largest chordwise extent of the four ice shapes. Figure 19 shows that there was less ice on the upper surface for the We_{DW}-based condition when compared to the *Re*-based method. The greater ice mass for the We_{DW} shape shown on Table 6 was due to the greater ice mass that formed on the lower surface, as shown on Figure 18. A predominate ridge of ice formed on the lower surface at the We_{DW} scaled condition for this case. This is similar to the ridge that formed in the Warm Hold case shown in Fig.14. It was likely an increase in the lower surface water loading produced by the angle of attack increase in conjunction with the elevated convective cooling resulting from the 60% increase in Reynolds number required by the We_{DW} scaling method produced an ice shape that was unexpected and

abnormal. Other than the large ice accretion on the lower surface for the We_{DW} condition, the other trends observed for the WSU Warm Hold scenario were similar to the other three scenarios shown previously.

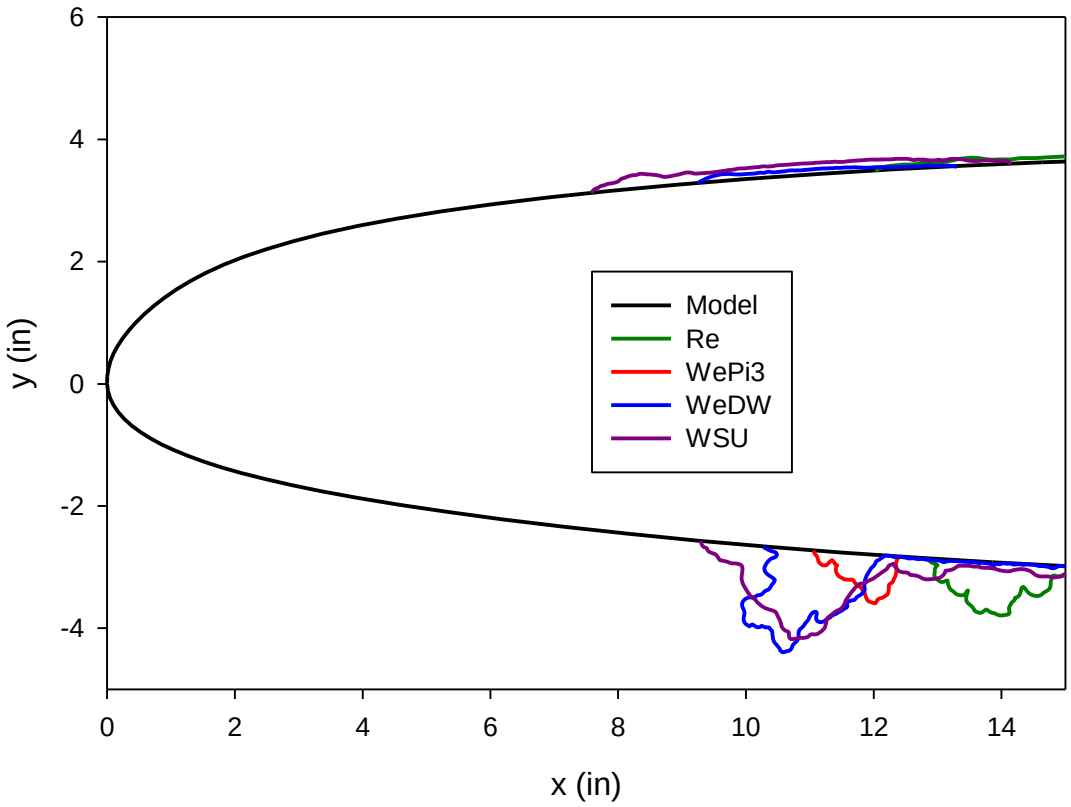

Figure 18. WSU Warm Hold scenario ice accretion tracing.

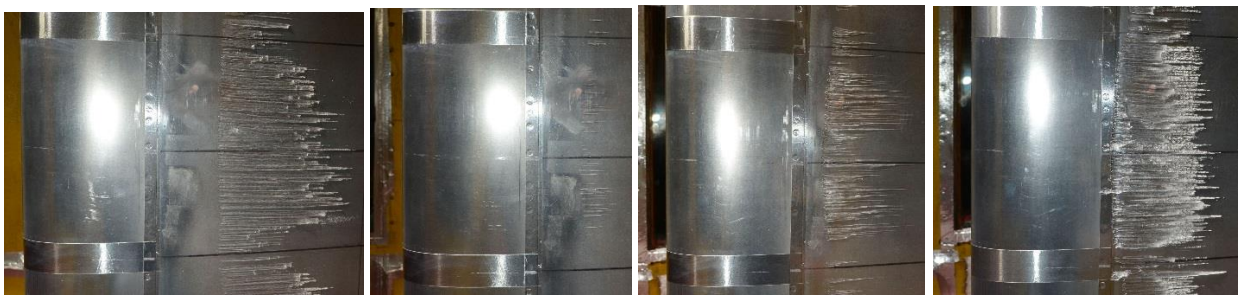

a) *Re* scaling **b) *WePi*3 Scaling** **c) We_{DW} Scaling** **d) WSU Scaling**

Figure 19. WSU Warm Hold scenario upper surface ice accretion.

The chordwise surface temperature distributions for the WSU Warm Hold scenario are shown in Fig. 20. The general trends are similar to what was shown for the other three scenarios in Figs. 8, 12, and 16. When the spray was on, the *WePi*3-based scaled condition had higher temperatures on the upper surface (downstream of the leading edge), when compared to other scaling methods. The *WePi*3-based scaling method had scaled water mass loading, unlike in the other scaling methods, resulting in less water mass hitting the upper surface, resulting in a slightly higher surface temperature. The large ice accretions on the lower surface of the other three scaling methods may have also been

large enough to alter the flowfield and increase the collection efficiency and water loading on the upper surface (when compared to the *WePi*3 condition). This may also have added to the discrepancy shown in Fig.20.

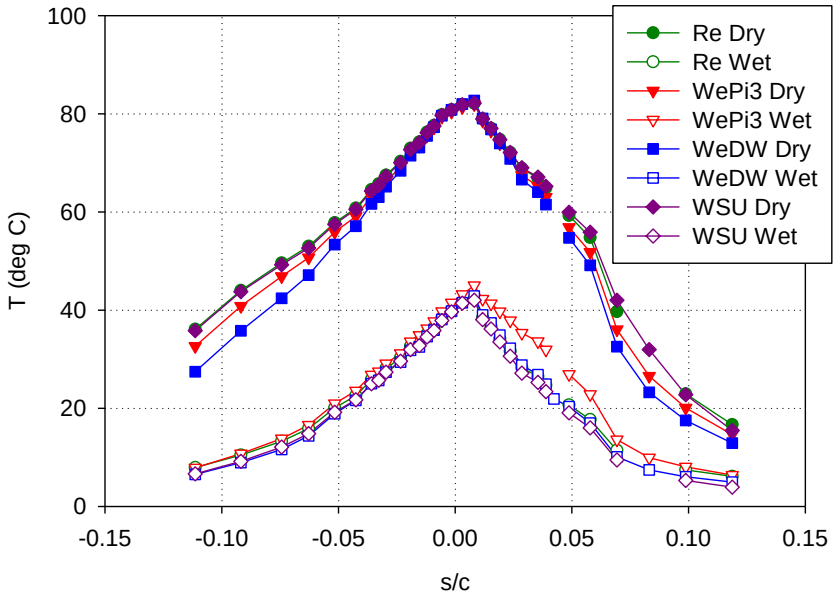

Figure 20. WSU Warm Hold scenario leading edge surface temperature.

Figure 21 shows the IPS heated air inlet/outlet temperatures and heated air energy input rates. The Re-scaling and WSU-scaling IPS inlet temperatures and energy input were nearly identical since they are similar scaling methods. Both of the *We*-based scaling inlet temperatures and energy input were higher than the *Re*-based scaling values, as expected.

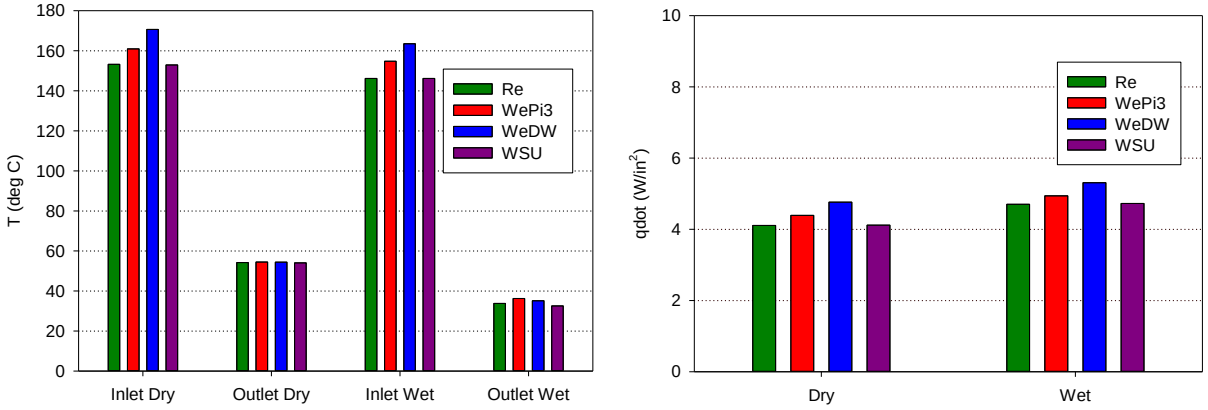

a) Heated air inlet/outlet temperature **b) Heated air energy input**

Figure 21. WSU Warm Hold scenario heated air temperature and energy input before and during icing exposure.

E. Comparison to AIWT Tests

The results of the IRT test largely agreed with and supported the results of the thermal IPS tests conducted at the AIWT. Trends in the amounts of ice accretion and their location and extent largely agreed with those observed at the AIWT. In two instances, a prominent ice ridge formed on the lower surface of the IRT model when operating under We_{DW} conditions. The larger (5 ft. chord vs. 1.5 ft. chord) asymmetric IRT model, when run at α greater than 0 degrees produced an increase in water loading on the lower surface which, in conjunction with the enhanced convective cooling resulting from the elevated Reynolds numbers generated by the We_{DW} scaling, resulted in not only a larger ice shape, but one exhibiting a change in character (i.e., the ice ridge).

F. Further Discussion

Three things can happen to water striking a heated aircraft surface in flight icing conditions: it can runback and freeze on an unheated or insufficiently heated surface, it can be re-entrained into the airstream, or it can be evaporated. The air pressure at flight altitudes affects all three of these modes of mass transport. Reynolds number scaling provides the surface temperature conditions for freezing of runback water, but does not provide similitude in either liquid water re-entrainment into the airstream or evaporation. The result is a great deal more ice being frozen on the surface than would occur at altitude conditions. Weber number based on water density scaling, in conjunction with surface temperature matching, provides the inertia to surface tension forces ratio needed to remove much of the excess water that is frozen in the Reynolds number scaling method. Because convective cooling is, however, much enhanced through the elevated Reynolds number generated by this method, excess ice can still result. The Weber number based on air density and $\pi 3$ method seeks to simulate all three modes of mass transport. Model surface temperature matching creates the surface condition for the ice to freeze in the proper location. Weber number based on air density matching generates ample inertia to surface tension forces to remove liquid water as would be the case at altitude, without over-enhancement of convective cooling through increased Reynolds number. Finally, the enhanced evaporation that occurs at altitude due to the decreased static pressure is addressed by reducing water loading in proportion to the reduction in calculated water evaporation rate.

IV. Conclusions

A test was conducted at NASA Icing Research tunnel to evaluate altitude scaling methods for thermal ice protection system. These methods were developed during a series of joint NASA/NRC-Canada tests at NRCC Altitude Icing Wind Tunnel using a small symmetric airfoil model. The IRT allowed these scaling methods to be evaluated on a larger asymmetric business jet airfoil with a more typical IPS design at higher Reynolds number.

The results from the IRT test largely agreed with and supported the results from the AIWT tests. The *We*-based scaling methods resulted in smaller runback ice mass than the *Re*-based scaling method. The *Re*-based scaling method generated runback ice that formed farther downstream than the *We*-based methods. These results agreed with those from the AIWT tests where the scale-method ice accretions were compared with reference (altitude) results. The Weber number based on air density coupled with surface temperature matching and water loading scaling produced the most consistent results. While not perfect, this method appears to be the best available to scale thermal IPS icing test conditions for altitude effects in an atmospheric icing wind tunnel. Moreover, they are not based on empirically-generated scale factors, but on fundamental physics. What is left is to better determine the limits of the physical relations used which can be accomplished by testing full-scale airfoil models in an altitude capable wind tunnel.

References

[1] SAE AIR6440, "Icing Tunnel Tests for Thermal Ice Protection Systems," SAE AC-9C Aircraft Icing Technology Committee, June 2014.

[2] Whalen, E.A., Broeren, A.P., and Bragg, M.B., "Characteristics of Runback Ice Accretions on Airfoils and their Aerodynamic Effects," 43rd AIAA Aerospace Sciences Meeting and Exhibit, January 10-13 2005, Reno, NV, AIAA Paper 2005-1065.

[3] Whalen, E.A., Broeren, A.P., and Bragg, M.B., "Characteristics of Runback Ice Accretions and their Aerodynamic Effects," FAA Report DOT/FAA/AR-07/16, April 2007.

[4] Papadakis, M., Wong, S.H., Yeong, H.W., Wong, S.C., and Vu, G.T., "Icing Tunnel Experiments with a Hot Air Anti-Icing System," 46th AIAA Aerospace Sciences Meeting and Exhibit, January 7-10, 2008, Reno, NV, AIAA Paper 2008-444.

[5] Addy, H.E., Oleskiw, M., Broeren, A.P., and Orchard, D., "A Study of the Effects of Altitude on Thermal Ice Protection System Performance," AIAA-2013-2934, NASA/TM-2013-216559.

[6] Addy, H.E., Orchard, D., Wright, W., and Oleskiw, M., "Altitude Effects on Thermal Ice Protection System Performance; a Study of an Alternative Approach," NASA/TM-2016-219081.

[7] Orchard, D.M., Addy, H.E., Wright, W.B., and Tsao, J., "Altitude Scaling of Thermal Ice Protection System in Running Wet Operation," 9th AIAA Atmospheric and Space Environments Conference, May 5-9, 2017, Denver, CO, (submitted for publication).

[8] Soeder, R.H., Sheldon, D.W., Ide, R.F., Spera, D.A. and Andracchio, C.R., "NASA Glenn Icing Research Tunnel User Manual," NASA TM-2003-212004, September 2003.